Supporting Information

Photophysical Properties and Kinetic Studies of 2-Vinylpyridine-Based Cycloplatinated(II) Complexes Containing Various Phosphine Ligands

Vahideh Dolatyari,[a] Hamid R. Shahsavari,[a]* Sepideh Habibzadeh,[b] Reza Babadi Aghakhanpour,[a]* Sareh Paziresh,[a] Mohsen Golbon Haghighi,[c] Mohammad Reza Halvagar[d]

[a] Department of Chemistry, Institute for Advanced Studies in Basic Sciences (IASBS), Zanjan, 45137-66731, Iran. Email: shahsavari@iasbs.ac.ir (H.R.S.); babadi@iasbs.ac.ir (R.B.A.).

[b] Department of Chemistry, Payame Noor University, P.O. BOX 19395-4697 Tehran, Iran

[c] Department of Chemistry, Shahid Beheshti University, Evin, Tehran 19839-69411, Iran.

[d] Department of Inorganic Chemistry, Chemistry and Chemical Engineering Research Center of Iran, Tehran 14968-13151, Iran.

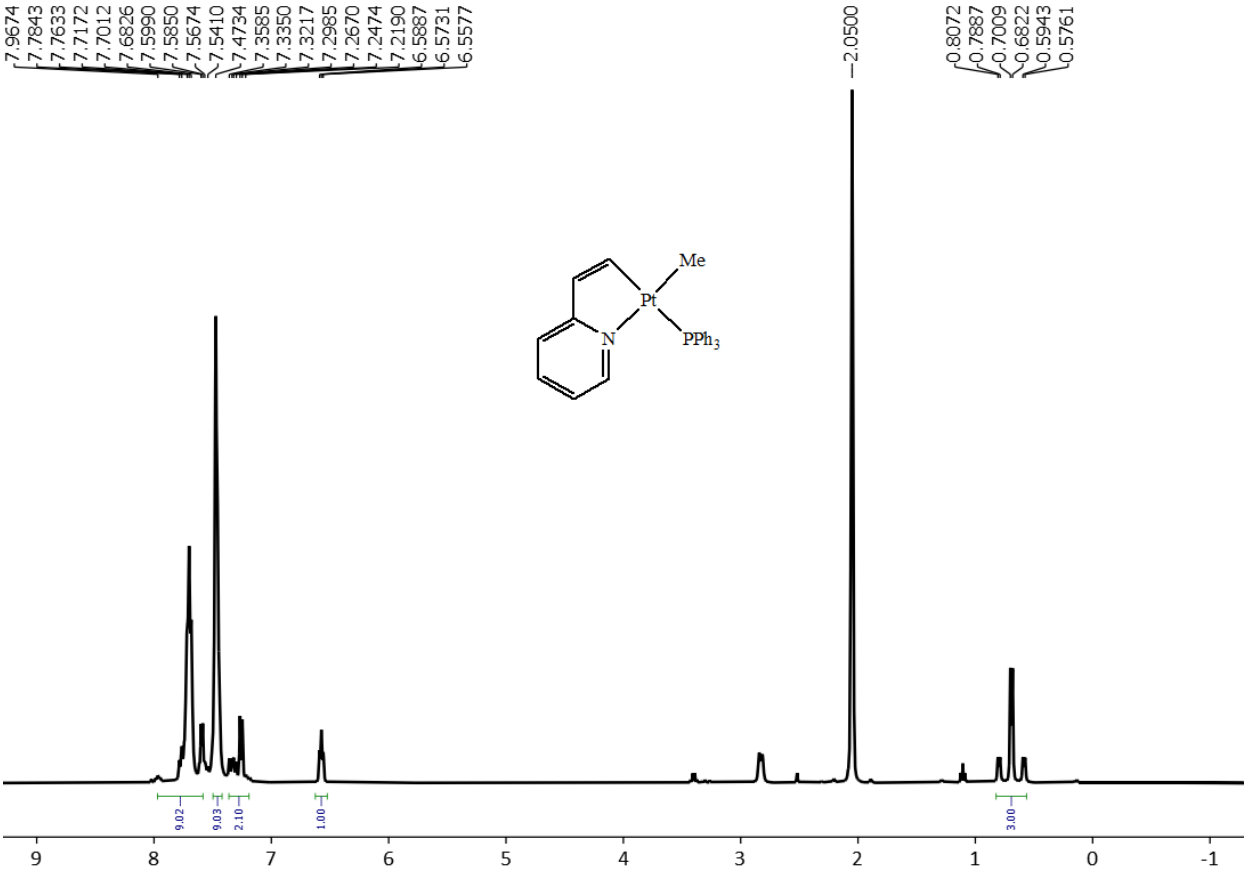

Figure S1. ^{1}H NMR spectrum of **1a** in acetone-d_6.

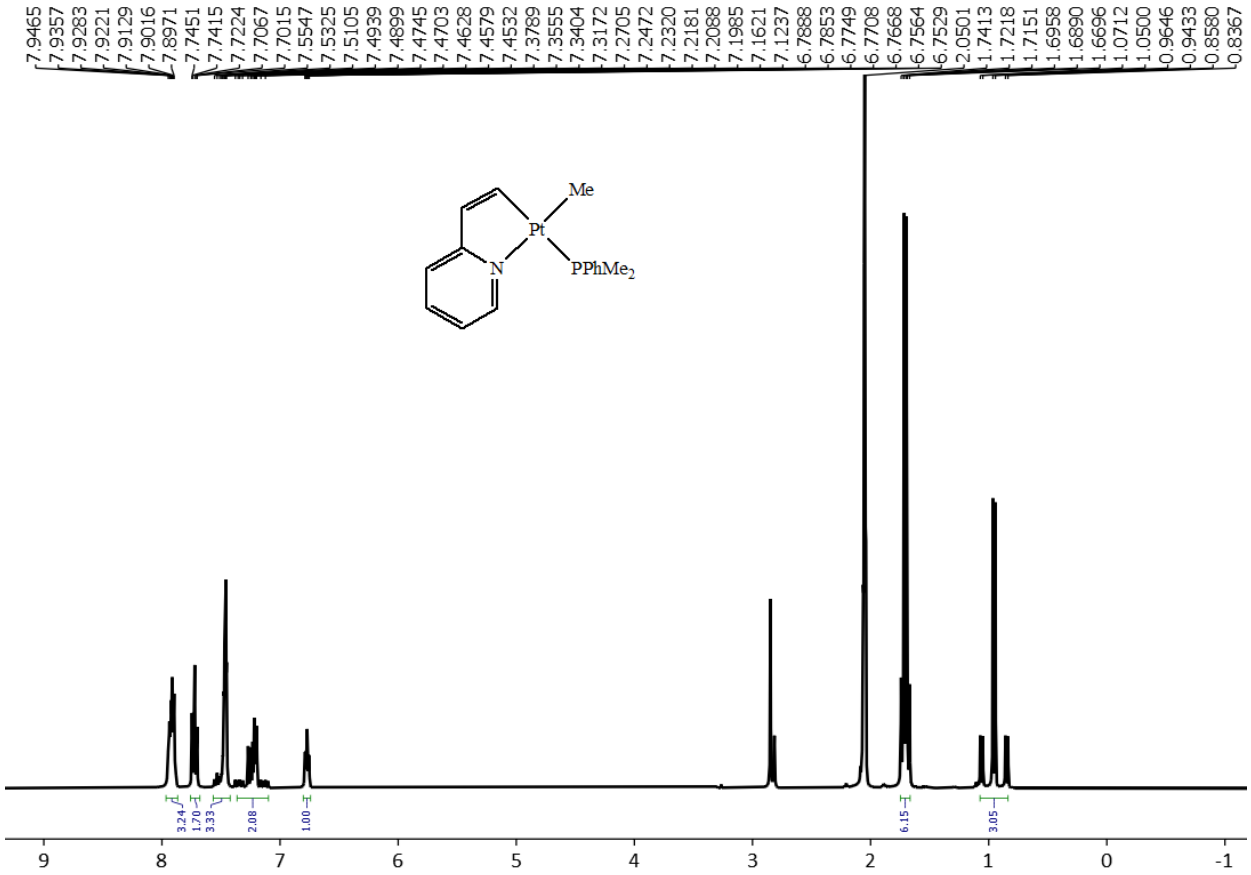

Figure S2. ^{1}H NMR spectrum of **1c** in acetone-d_6.

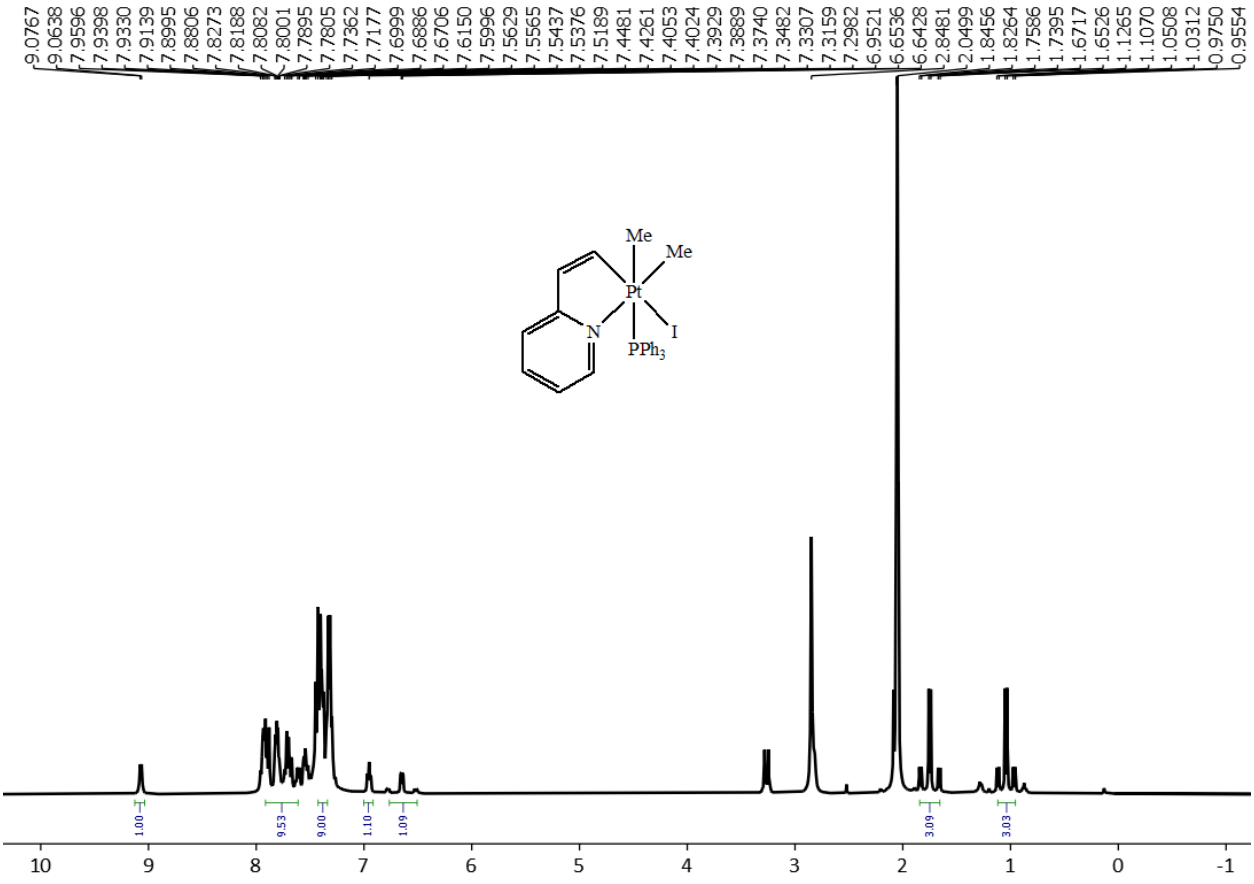

Figure S3. ^{1}H NMR spectrum of **3a** in acetone-d_6.

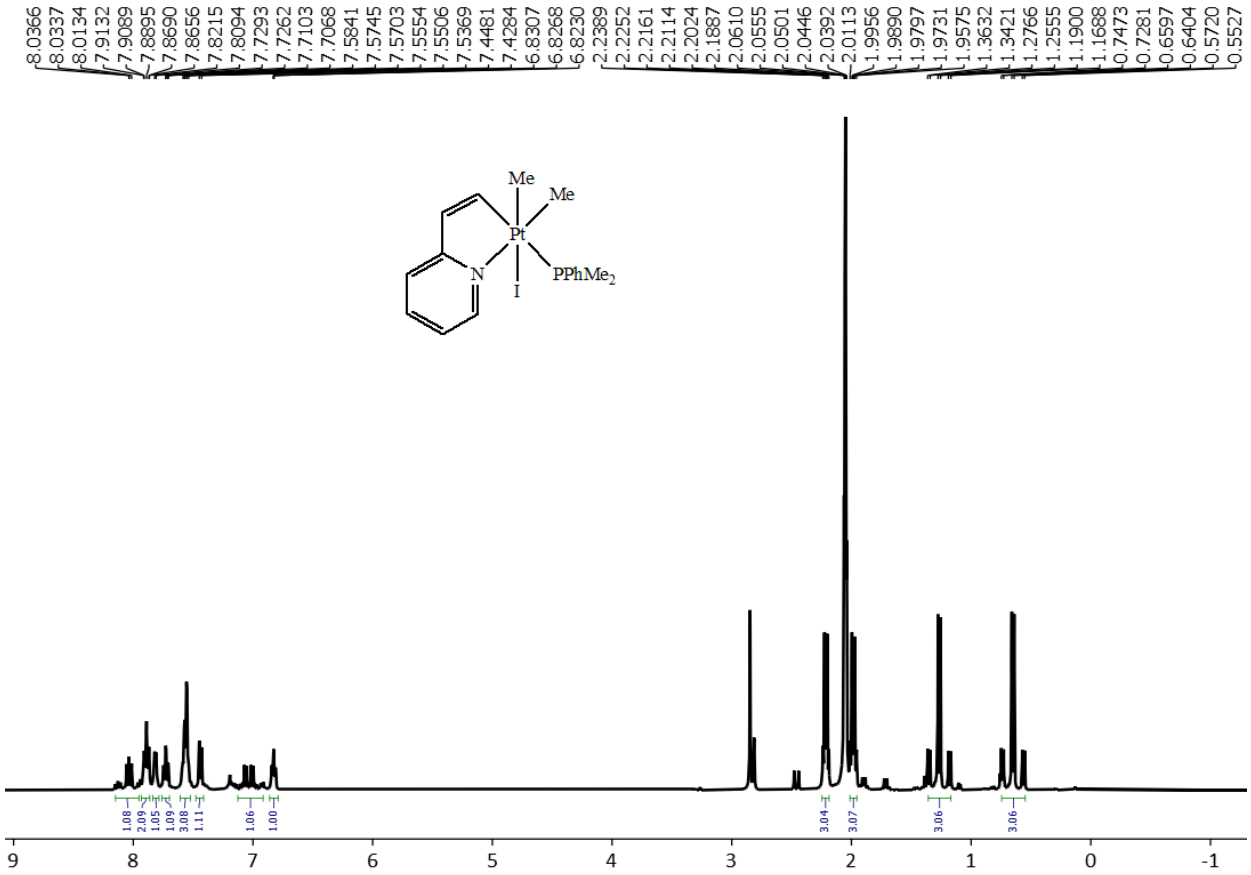

Figure S4. ^{1}H NMR spectrum of **2c** in acetone-d_6.

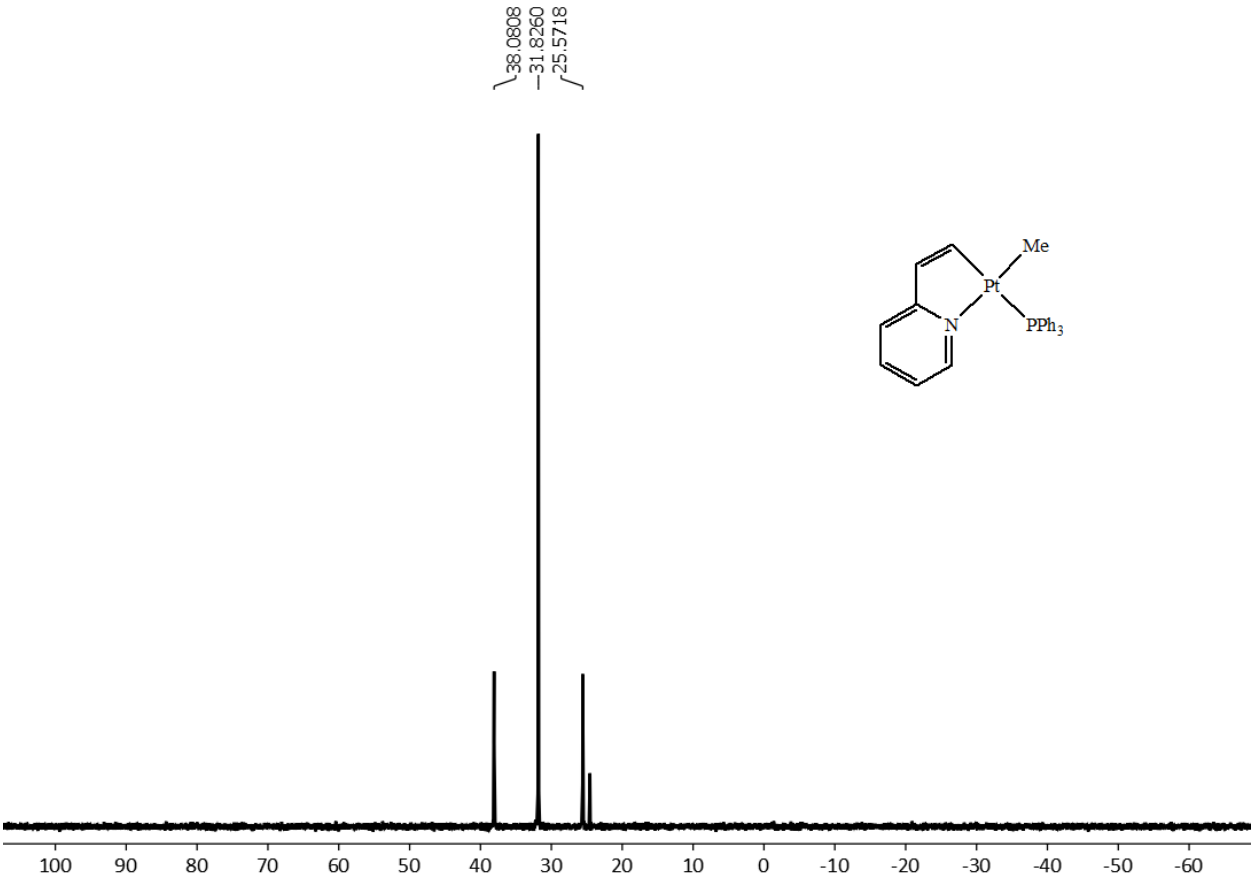

Figure S5. $^{31}P\{^{1}H\}$ NMR spectrum of **1a** in acetone-d_6.

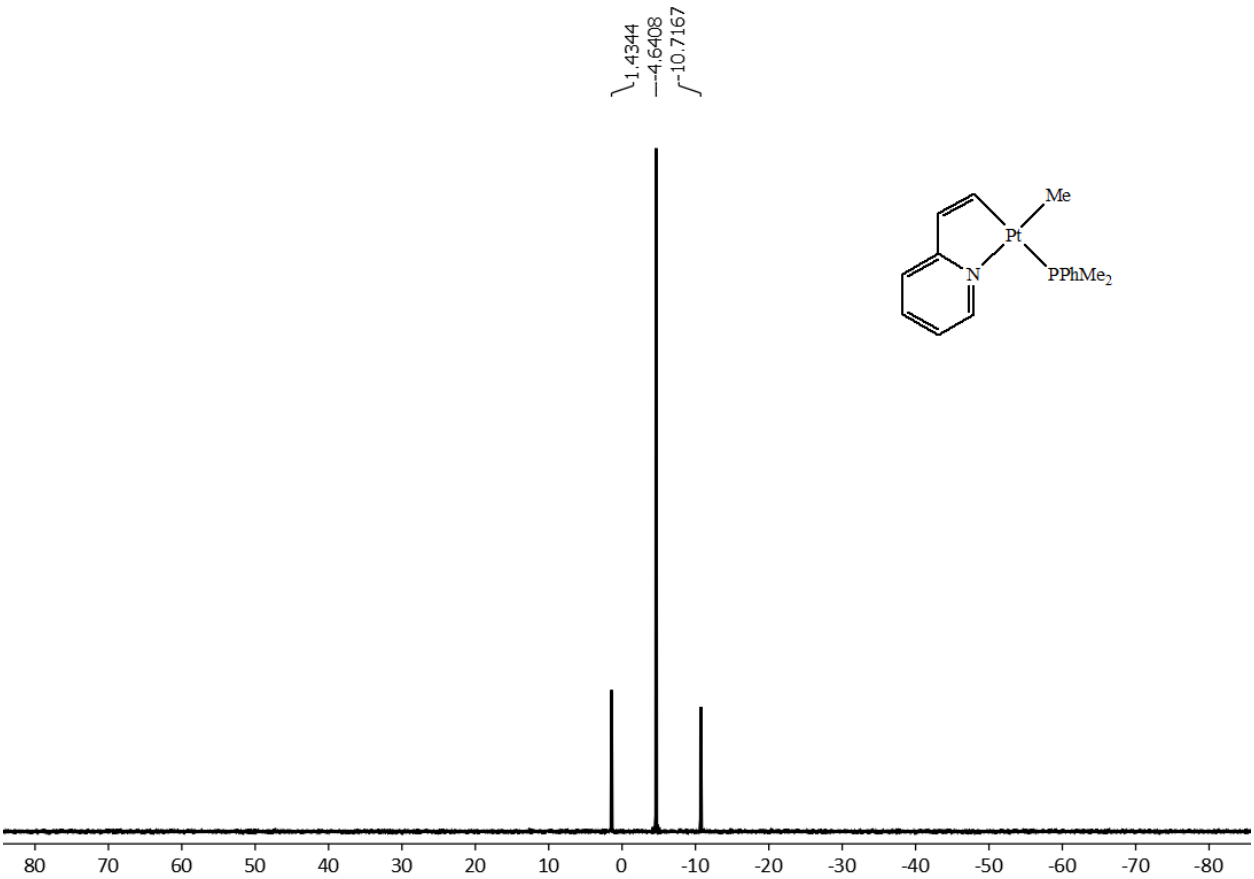

Figure S6. $^{31}P\{^{1}H\}$ NMR spectrum of **1c** in acetone-d_6.

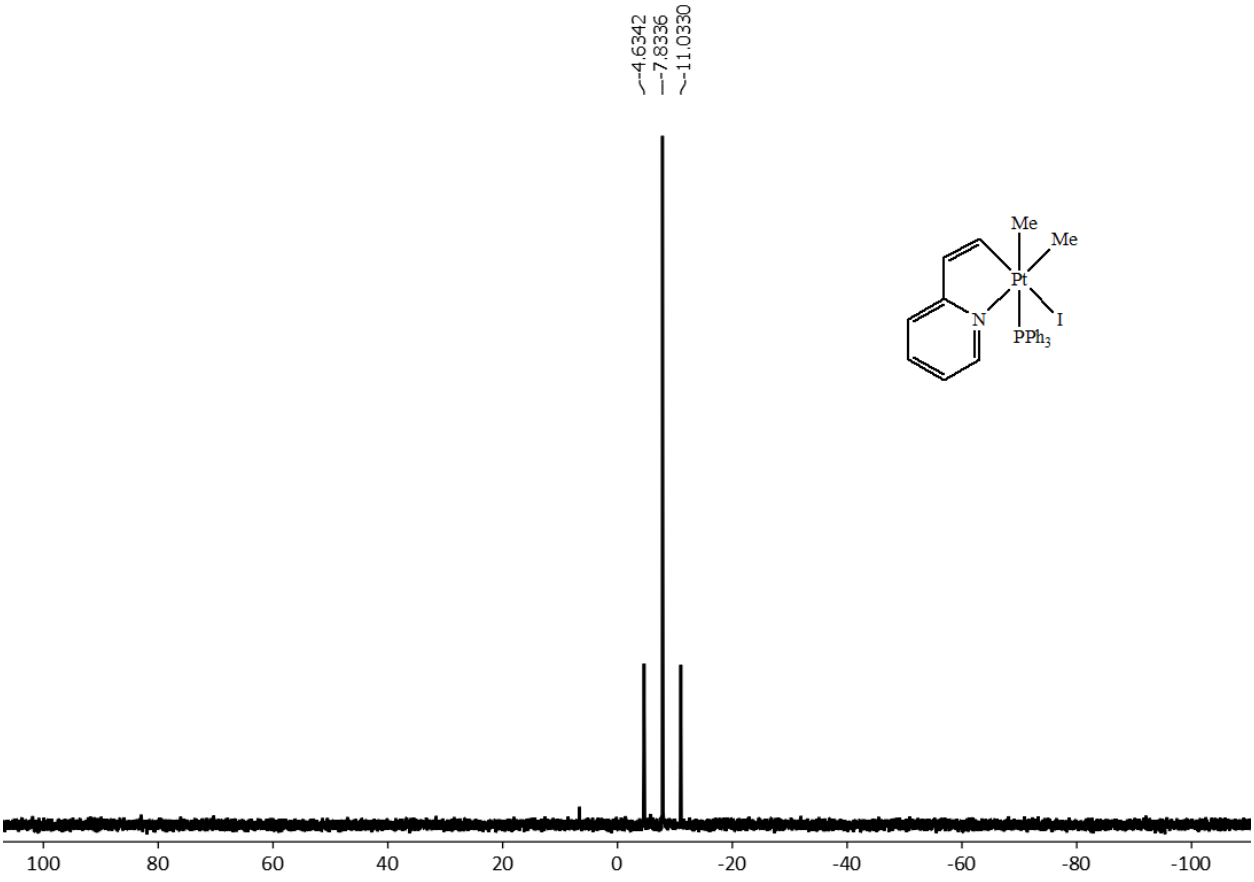

Figure S7. $^{31}P\{^{1}H\}$ NMR spectrum of **3a** in acetone-d_6.

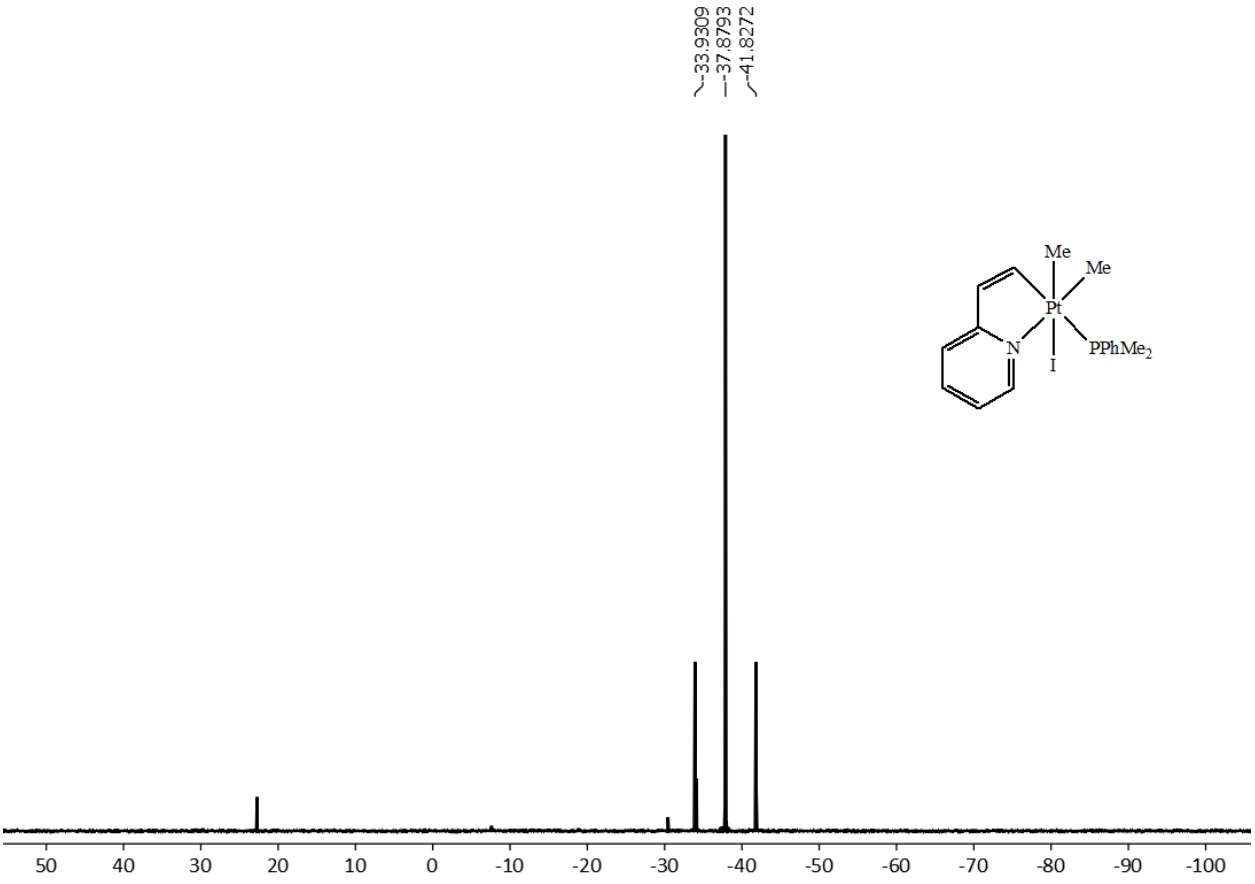

Figure S8. $^{31}P\{^{1}H\}$ NMR spectrum of **2c** in acetone-d_6.

Table S1. Crystal data and structure refinements for **1c** and **2c**.

	1c	**2c**
Formula	$C_{16}H_{20}NPPt$	$C_{17}H_{23}INPPt$
Formula weight	452.39	594.32
T, K	294(2)	294(2)
Crystal system	Monoclinic	Monoclinic
Space group	P21/n	P21/c
a (Å)	12.397(3)	12.783(3)
b (Å)	8.8869(18)	10.555(2)
c (Å)	14.831(3)	14.278(3)
α (deg)	90	90
β (deg)	95.81(3)	94.29(3)
γ (deg)	90	90
Z	4	4
Volume, $Å^3$	1625.6(6)	1921.1(7)
Density, g/m^3	1.849	2.055
Data / restraints / parameters	2863 / 0 / 175	3168 / 175 / 193
Goodness-of-fit on F^2	0.502	0.661
R(*F* obsd data)	*R*1 = 0.0254	*R*1 = 0.0578
wR(F^2 all data)	*wR*2 = 0.0405	*wR*2 = 0.1442
CCDC No.	2057874	2057873

$R1 = \Sigma \, ||F_o| - |F_c|| \, / \, \Sigma \, |F_o|$

$wR2 = \{ \, \Sigma \, [w(F_o^2 - F_c^2)^2] \, / \, \Sigma \, [w(F_o^2)^2] \, \}^{1/2}$

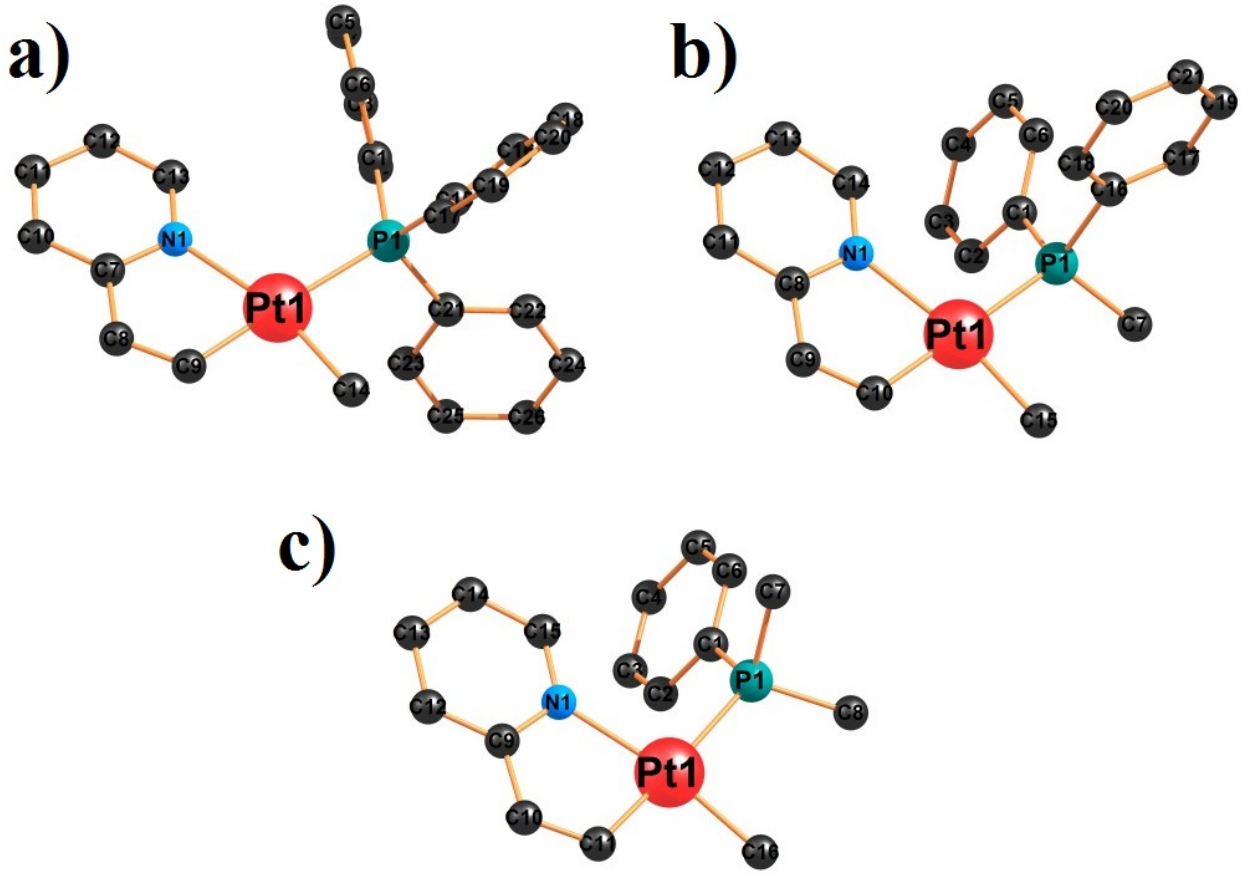

Figure S9. Optimized structures of a) **1a**, b) **1b** and c) **1c** in CH_2Cl_2 solvent.

Table S2. Selected geometrical parameters for the optimized structures of **1a-1c**.

1a	1b	1c
Pt1-P1 2.43015	Pt1-P1 2.41912	Pt1-P1 2.40937
Pt1-N1 2.24333	Pt1-N1 2.24359	Pt1-N1 2.23517
Pt1-C9 2.01262	Pt1-C10 2.01298	Pt1-C11 2.01418
Pt1-C14 2.07504	Pt1-C15 2.06778	Pt1-C16 2.06659
C9-Pt1-N1 77.94346	C10-Pt1-N1 77.99727	C11-Pt1-N1 78.12800
N1-Pt1-P1 104.65230	N1-Pt1-P1 101.12916	N1-Pt1-P1 99.30456
P1-Pt1-C14 89.37497	P1-Pt1-C15 89.74736	P1-Pt1-C16 90.95920
C14-Pt1-C9 88.05046	C15-Pt1-C10 91.15671	C16-Pt1-C11 91.59204
C9-Pt1-P1 177.31292	C10-Pt1-P1 178.41196	C11-Pt1-P1 176.47379
N1-Pt1-C14 165.88684	N1-Pt1-C15 169.05832	N1-Pt1-C16 169.71877

Table S3. Composition (%) of frontier MOs in the ground state for **1a** in CH_2Cl_2 solvent.

MO	Energy (eV)	Components (%)			
		Pt	Me	Vpy	PPh_3
LUMO+5	-0.414	1	0	19	80
LUMO+4	-0.532	4	1	1	94
LUMO+3	-0.621	8	1	53	38
LUMO+2	-0.757	10	1	16	73
LUMO+1	-0.917	4	0	5	91
LUMO	-1.472	11	1	77	11
HOMO	-5.608	42	0	54	4
HOMO-1	-5.812	85	3	8	4
HOMO-2	-6.110	86	3	8	3
HOMO-3	-6.411	14	1	22	62
HOMO-4	-6.687	72	9	12	7
HOMO-5	-6.955	3	1	4	92

Table S4. Composition (%) of frontier MOs in the ground state for **1b** in CH_2Cl_2 solvent.

MO	Energy (eV)	Components (%)			
		Pt	Me	Vpy	PPh_2Me
LUMO+5	-0.205	3	0	5	92
LUMO+4	-0.366	1	4	7	88
LUMO+3	-0.559	8	1	18	74
LUMO+2	-0.628	5	0	66	29
LUMO+1	-0.842	3	0	3	94
LUMO	-1.476	11	2	80	7
HOMO	-5.601	41	0	55	3
HOMO-1	-5.829	87	3	7	3
HOMO-2	-6.095	87	6	7	0
HOMO-3	-6.496	17	3	27	53
HOMO-4	-6.723	71	8	10	11
HOMO-5	-7.029	2	1	1	96

Table S5. Composition (%) of frontier MOs in the ground state for **1c** in CH_2Cl_2 solvent.

MO	Energy (eV)	Components (%)			
		Pt	Me	Vpy	$PPhMe_2$
LUMO+5	0.799	30	17	28	25
LUMO+4	0.428	39	2	27	33
LUMO+3	-0.293	5	0	5	89
LUMO+2	-0.636	3	0	80	17
LUMO+1	-0.696	4	0	12	84
LUMO	-1.485	11	2	82	6
HOMO	-5.599	41	0	55	3
HOMO-1	-5.838	88	3	7	2
HOMO-2	-6.095	87	6	7	0
HOMO-3	-6.539	36	6	25	34
HOMO-4	-6.804	55	6	17	21
HOMO-5	-7.056	5	0	3	92

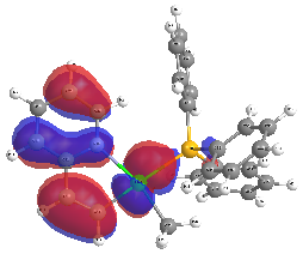	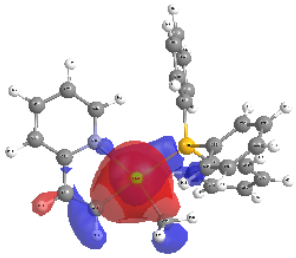	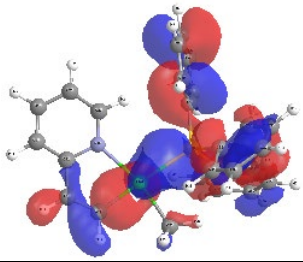
HOMO	**HOMO-1**	**HOMO-2**
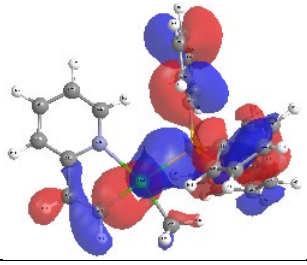	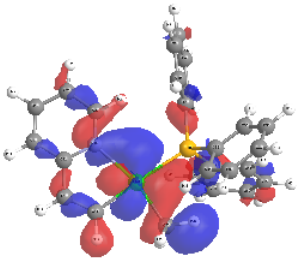	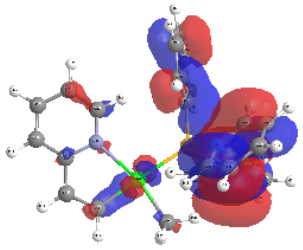
HOMO-3	**HOMO-4**	**HOMO-5**
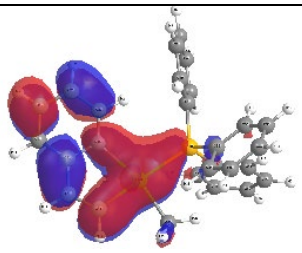	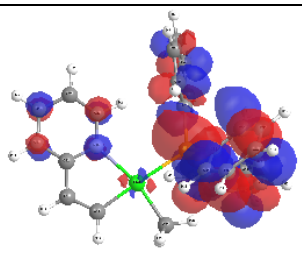	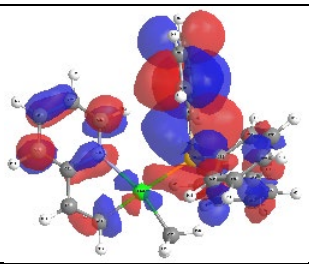
LUMO	**LUMO+1**	**LUMO+2**
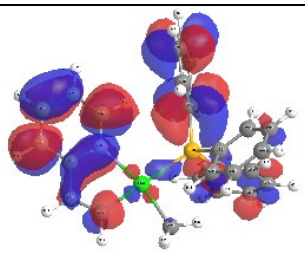	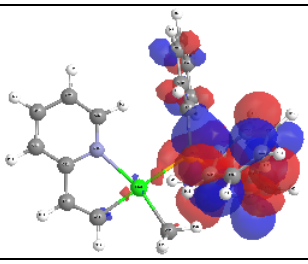	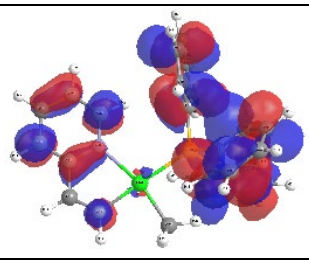
LUMO+3	**LUMO+4**	**LUMO+5**

Figure S10. Selected MO plots of **1a**.

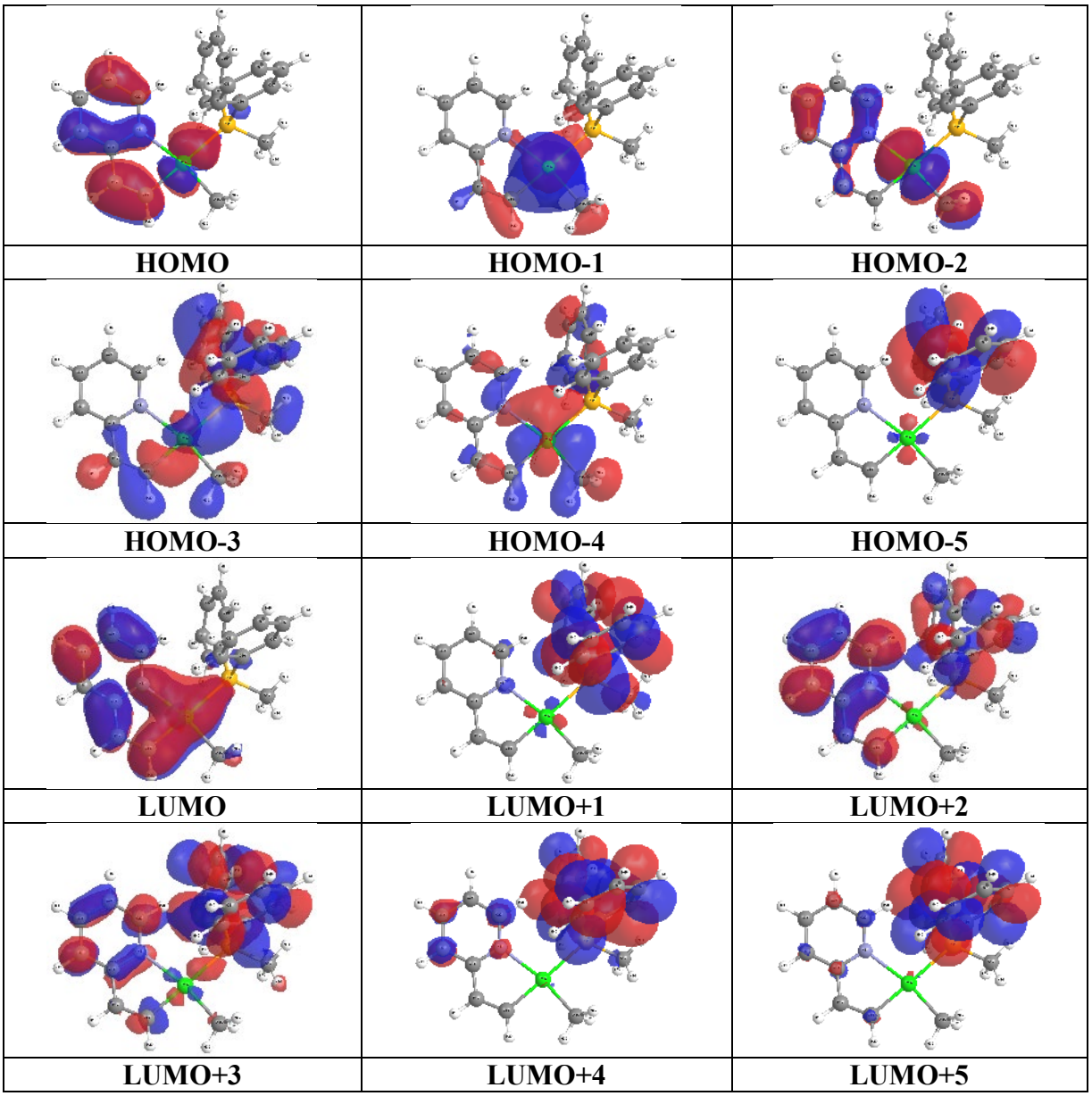

Figure S11. Selected MO plots of **1b**.

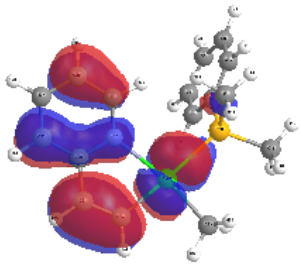	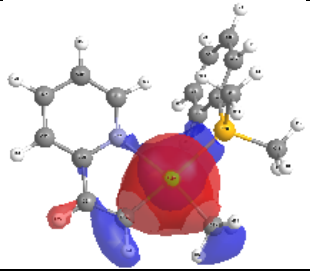	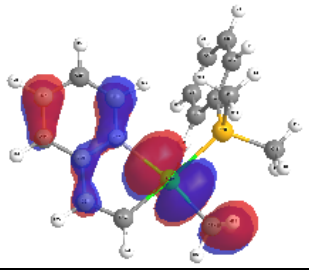
HOMO	**HOMO-1**	**HOMO-2**
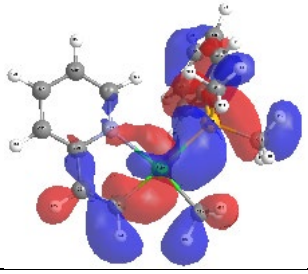	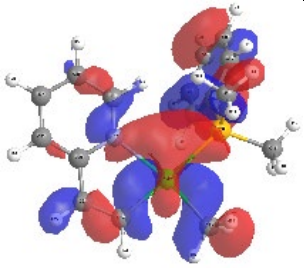	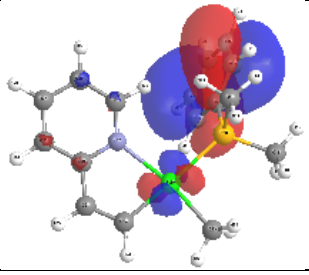
HOMO-3	**HOMO-4**	**HOMO-5**
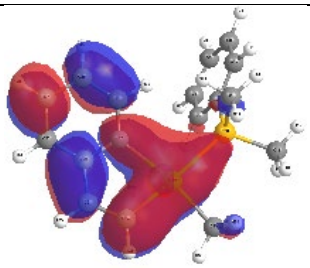	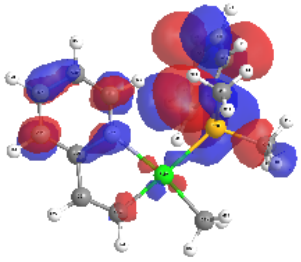	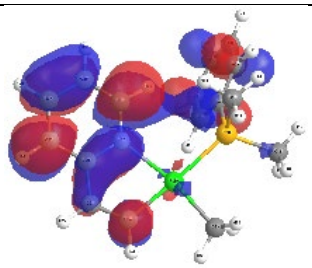
LUMO	**LUMO+1**	**LUMO+2**
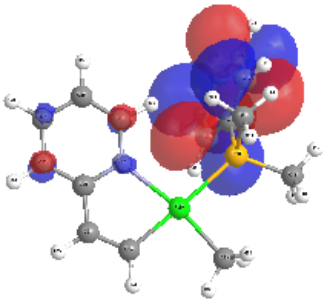	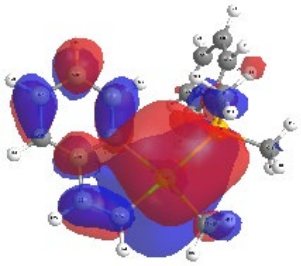	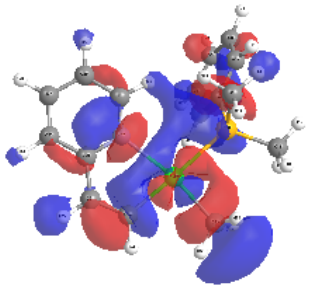
LUMO+3	**LUMO+4**	**LUMO+5**

Figure S12. Selected MO plots of **1c**.